Journal of Applied Sciences

ISSN 1812-5654

science alert

ANSInet
an open access publisher
http://ansinet.com

Journal of Applied Sciences 9 (13): 2381-2389, 2009
ISSN 1812-5654

Signal Processing Method for Evaluating Fatigue Damage in a Piping System

S. Abdullah, M. Loman and N. Jamaluddin
Department of Mechanical and Materials Engineering, Faculty of Engineering and Built Environment,
Universiti Kebangsaan Malaysia, 43600 Bangi, Selangor, Malaysia

Abstract: This study focuses on the assessment of fatigue damage in a piping system. Strain loading data was acquired using the fatigue data acquisition devices on a lab scale piping system. Specifically, the data was measured on the roughened and smooth pipe surfaces simultaneously, where the strain gauges were mounted on both of the piping surfaces. In this study, three different water flow rates were operated in the experiments which were normal, maximum and variable. The normal water flow rate was assumed as the reference flow rate for the subsequent fatigue analysis. The recorded strain signal was then analyzed using the frequency and time-frequency method and the short-time Fourier transform was applied to explain the fatigue damage events. The fatigue data from the experiment was employed to calculate the fatigue damage of the piping system.

Key words: Fatigue damage, strain loading, flow rates, time-frequency analysis, short-time Fourier transform

INTRODUCTION

To assure safe and reliable service life but also for an optimized maintenance strategy, it is necessary to have a precise estimation of lifetime consumption of critical components. A life monitoring system is usually understood as a computerized system which takes data from transducers fitted to a piece of plant and calculates on-line the theoretical creep and fatigue damage experienced by the plant due to operation and hence, the remanent life of the plant. These systems have historically been fitted mainly to large boiler plant but are applicable to other high temperature plant as well (Majle *et al*., 1996). It is important to evaluate structural integrity of highly pressurized piping for power plants. The wall thickness of a pressurized pipe is designed to satisfy a corrosion margin (Miyazaki, 2002). A study of fatigue damage is necessarily done since single pipe damage could not be detected unless the whole piping system must be replaced with the new one. The signal processing method was used in this study in order to create an estimation system of fatigue failure detection.

Fatigue is a localized damage process of a component produced by cyclic loading. It is the cumulative process consisting of crack initiation, propagation and final fracture of component. During cyclic loading, localized plastic deformation may occur at the highest stress site. This plastic deformation induces permanent damage to the component and a crack develops. As the component experiences an increasing number of loading cycles, the length of the crack also increases. After a certain number of cycles, the crack will cause the component to fail (Lee *et al*., 2005). The fatigue damage starts when the component goes into service and is subjected to some form of cyclic stress. As the material is subjected to repeated cyclic loads, additional fatigue damage occurs. This fatigue damage is cumulative in nature and progresses until a fatigue crack forms. If the crack is not detected by inspection and the affected equipment is placed back into service, the crack grows until the component fails by leak, brittle fracture, or gross plastic deformation due to overload of the remaining cross sectional area (Gokhale *et al*., 2007).

Current industrial practice for fatigue life prediction is to use the Palmgren-Miner (PM) linear damage rule (Abdullah *et al*., 2005). For the strain-based fatigue life prediction, this rule is normally applied with strain-life fatigue damage models. The first strain-life model is the Coffin-Manson relationship, i.e.:

$$\varepsilon_a = \frac{\sigma_f^{'}}{E}(2N_f)^b + \varepsilon_f^{'}(2N_f)^c \quad (1)$$

where, E is the material modules of elasticity, ε_a is a true strain amplitude, $2N_f$ is the number of reversals to failure, ε'_f is a fatigue strength coefficient, b is a fatigue strength exponent, ε'_f is a fatigue ductility coefficient and c is a fatigue ductility exponent.

In designing for durability,the presence of non zero mean stress can influence fatigue behavior of materials

Corresponding Author: Shahrum Abdullah, Department of Mechanical and Materials Engineering, Faculty of Engineering and Built Environment, Universiti Kebangsaan Malaysia, 43600 Bangi, Selangor, Malaysia Tel: 603-89216518 Fax: 603-89216145, 603-89259659

because a tensile or a compressive normal mean stress has been shown to be responsible for accelerating or decelerating crack initiation and growth (Lee *et al*., 2005). In conjunction to the local strain life approach, many models have been proposed to quantify the effect of mean stresses on fatigue behavior. Morrow (Morrow, 1968) has proposed the following relationship when a mean stress is present:

$$\varepsilon_a = \frac{\sigma_f^{'}}{E}\left(1-\frac{\sigma_m}{\sigma_f^{'}}\right)(2N_f)^b + \varepsilon_f^{'}(2N_f)^c \quad (2)$$

Equation 2 implies the mean normal stress can be taken into account by modifying the elastic part of the strain-life curve by the mean stress, σ_m. Equation 2 has been extensively cited for steels and used with considerable success in the long-life regime when plastic strain amplitude is of little significance.

Smith *et al*. (1970) proposed a method that assumes that the fatigue damage in a cycle is determined by $\sigma_{max}\ \varepsilon_a$, where σ_{max} is the maximum tensile stress and ε_a is the strain amplitude. Also, the SWT parameter is simply a statement of $\sigma_a\varepsilon_a$ for a fully reversed test is equal to $\sigma_{max}\ \varepsilon_a$ for a mean stress test. The SWT parameter predicts no fatigue damage if the maximum tensile stress becomes zero and negative. The SWT mean stress correction formula is expressed as follows:

$$\sigma_{max}\varepsilon_a = \frac{\left(\sigma_f^{'}\right)^2}{E}(2N_f)^{2b} + \sigma_f^{'}\varepsilon_f^{'}(2N_f)^{b+c} \quad (3)$$

For loading sequences that are predominantly tensile, the SWT approach is more conservative and therefore recommended. In a case of the loading being predominantly compressive, particularly for wholly compressive cycles, the Morrow model provides more realistic life estimates (Dowling, 1999). Generally, the selection of mean stress correction approach highly based on the value of mean stress itself as well as the material. For instance, the unmodified Morrow approach seem to work reasonably well for steels and in at least some cases gives better results than the SWT parameter (Dowling, 1999). However, the SWT model appears to work particularly well for aluminum alloy, cast iron, hardened carbon steel and microalloy steels (Lee *et al*., 2005). According to Lee *et al*. (2005), the mean stress correction approach are empirically calculated and it should be compared to the test data in order to determine the most appropriate model for a specific material and test condition.

The signal processing methods were utilised in order to analyze the time domain raw data. The frequency analysis is performed in order to convert a time domain signal into the frequency domain. The results of a frequency analysis are most commonly presented by means of graph having frequency on the x-axis and amplitude on the y-axis. The Fourier analysis is a one of the method to analyze random data based on the frequency domain analysis. The algorithm that is used to split the time history into its constituent sinusoidal components is the Fourier transform. This transform was first defined by the French mathematician and engineer Jean Baptiste Joseph Fourier who postulated that any periodic function could be expressed as the summation of sinusoidal waves of varying frequency, amplitude and phase. Smith (1999) defined spectral analysis as understanding a signal by examining the amplitude, frequency and phase of its component sinusoids. For a periodic time function, x (t), frequency analysis can be performed using the classical Fourier transform defined by the mathematical definition:

$$X(\omega) = \frac{1}{2\pi}\int_{-\infty}^{\infty} x(t)e^{-i\omega t}dt \quad (4)$$

where, X(ω) is the amplitude of Fourier transform in frequency distribution, ω is the angular frequency and f_k.

The frequency analysis data is typically presented in graphical form as Power Spectral Density (PSD). A PSD is a normalized density plot describing the mean square amplitude of each sinusoidal wave with respect to its frequency. The PSD presents the vibrational energy distribution of the signal across the frequency domain. Each frequency step value of the PSD is characterized by amplitude, A_k, defined as:

$$A_k = \sqrt{2\Delta f \cdot S(f_k)} \quad (5)$$

where, $S(f_k)$ is the underlying PSD of the signal and f_k is the harmonic frequency.

The PSD can be as an input for generating a time-varying signal by performing the IDFT or IFFT. However, the time series which was generated from IFFT is not as accurate as the original signal because the PSD does not contain the original signal phase information. The assumptions of the signal phase content can be made in order to regenerate a statistically equivalent time history. For example, if the time history is taken from an ergodic stationary for Gaussian and random process, the phase is purely random between -π and +π radians (Halfpenny, 1999; Li *et al*., 2001).

The Short-Time Fourier Transform (STFT) is a method of time-frequency analysis which aims to produce frequency information which has a localization in time.

The STFT is performed by dividing the signal into small sequential or overlapping data frames, for which the Fast Fourier Transform (FFT) was applied to each data frame (Kiymik *et al*., 2005). It provides information about when and at what frequencies a signal event occurs. The STFT approach assumes that if a time-varying signal is divided into several segments, each can be assumed stationary for analysis purposes. The Fourier transform is applied to 24 each of the segments using a window function, which is typically nonzero in the analyzed segment and is set to zero outside. The most important parameter in the analysis is the window length, which is chosen so as to isolate the signal in time without any distortions. The STFT was developed from the Fourier transform and it is mathematically defined as:

$$STFT = X(\tau,\omega) = \int_{-\infty}^{\infty} \omega(t-\tau)e^{-\omega x} x \quad (6)$$

where, the Fourier transform of the windowed signal is $x(t)e^{-i\omega t}$, ω is the frequency and τ is the time position of the window (Chui, 1991).

The time-frequency resolution depends on the selection of the window length. The time window length is defined as Δt and the frequency bandwidth is $\Delta\omega$. Considering the relationship between time and frequency, i.e.:

$$\Delta\omega = 1/\Delta t \text{ or } \Delta\omega\Delta t = 1 \quad (7)$$

It can be seen that a good time localization (when Δt is small) or frequency localization (when $\Delta\omega$ is small) can be obtained, but not both simultaneously. Therefore, the time window length Δt and the frequency bandwidth $\Delta\omega$ are interrelated.

MATERIALS AND METHODS

In this study, the strain signal was measured on a laboratory scale water piping system as shown in Fig. 1. Two control valves which each valve located at each pipe were used to open, close and control the flow rate. In this case, both control valves were set up to the similar conditions in order to gain related signals for the particular pipe surfaces. The sections measured were the two horizontal pipes of the same outer diameter but with different internal surface features which were roughened and smooth surfaces at three different flow rates. Two different types of internal surface; smooth and roughened were utilised in order to compare the results for fatigue damage, energy and other features. These two different surfaces were chosen based on the assumption that the results may vary due to the difference of internal surfaces of the pipe. The fatigue data acquisition system was used for the strain signal measurement.

Two millimeter in size strain gauges were used for measuring the strain loading signals. The strain gauges were mounted on the mirror-polished pipes intentionally in the same direction of the water flow. For this reason, the strain gauges can detect any deformation occurs on the pipe surface. The signals were estimated to be the Variable Amplitude (VA) loading which was then sampled at 50 Hz. The measured strain signals were shown in Fig. 2. For the post processing stage, the GlyphWorks®

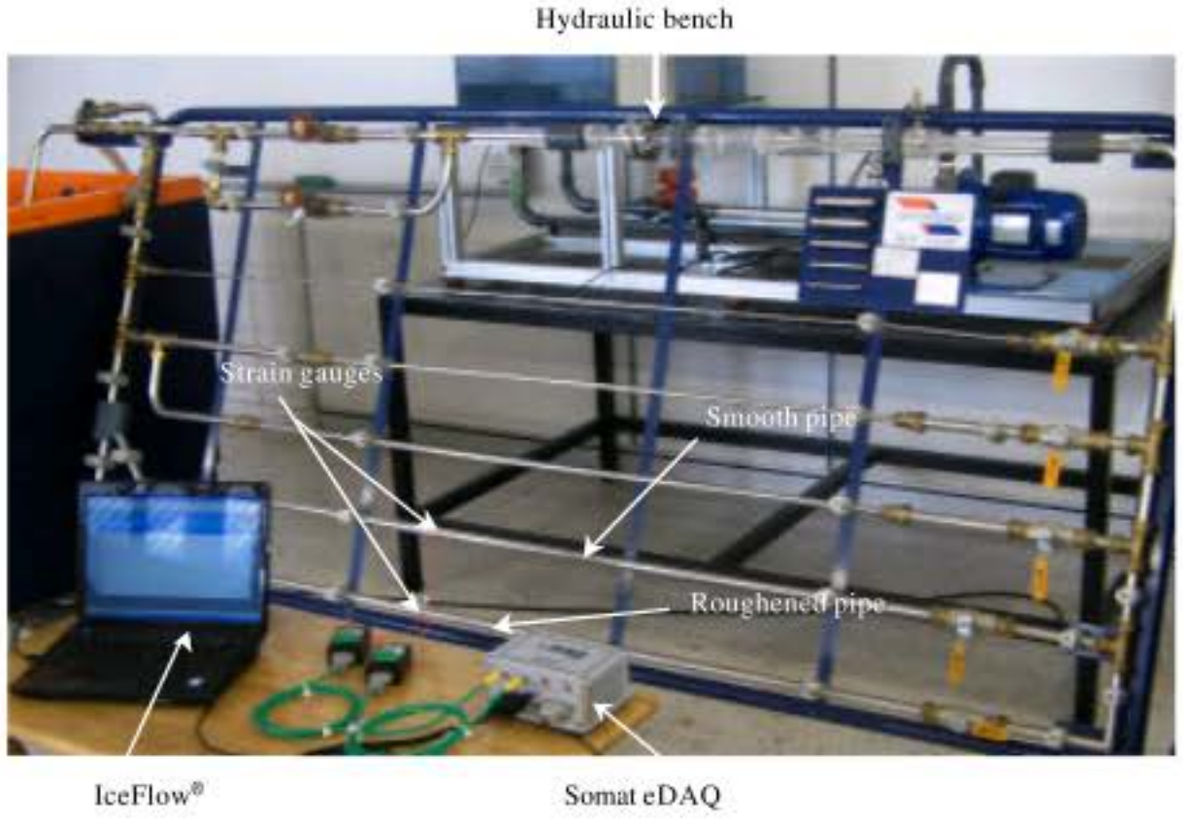

Fig. 1: Test rig set up for strain data measurement

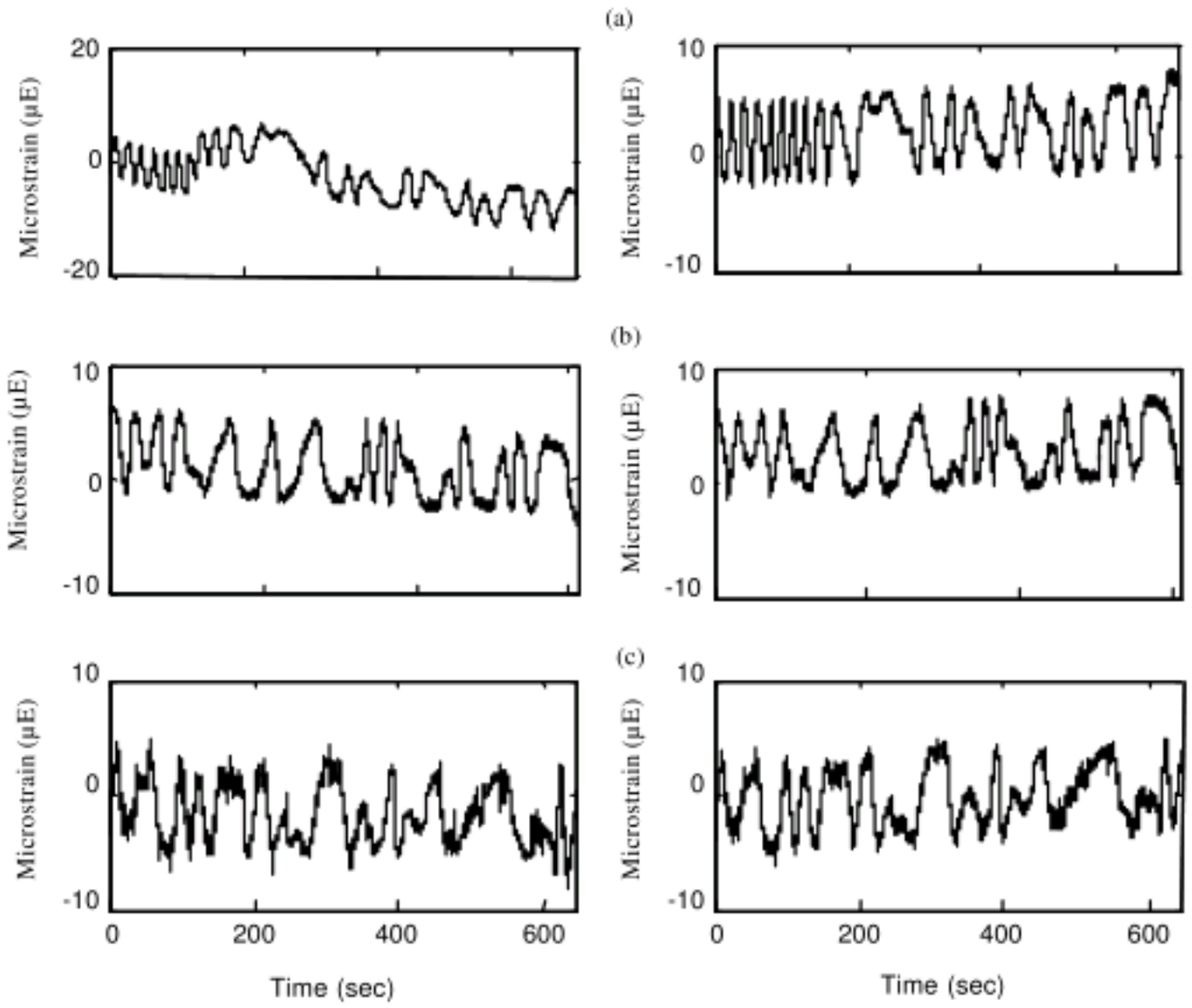

Fig. 2: The original strain signal for smooth (left side) and roughened (right side) pipe at: (a) normal flow rate, (b) maximum flow rate and (c) variable flow rate

software package was used to calculate the fatigue damage of the pipes and the Matlab® software was also used to analyze the signal processing approach.

RESULTS AND DISCUSSION

Frequency analysis: Several methods in signal processing have been utilised to process the data obtained during the test. The Power Spectral Density method was used to convert the time domain signal into the frequency domain. It indicated each of frequency existed in the signal. The distribution of vibrational signal energy across the frequency domain can be observed using this method. The plot of PSD for roughened pipe surface can be shown in Fig. 3. As shown in Fig. 3, the frequency for roughened pipe is lower than 0.2 Hz. It means that the fatigue damage in pipe occurs at low frequencies.

Time-frequency analysis: The time domain signal was converted into time-frequency domain using the STFT method. This method allows us to determine the value of frequency at a particular time. High amplitude events in time domain signal was represented by the narrow and wide band power spectrums in the time-frequency representation. It can be seen clearly in Fig. 4 for which the narrow band signals in the original time history occurred as a number of events with narrow bandwidths in the time-frequency mapping added with frequency information. Similarly, wide band signals in time history occurred as wide power spectrum in STFT as in red circle.

Figure 5 and 6 show the examples of time-frequency representation of the smooth and roughened pipe surfaces at normal, maximum and variable flow rates. The characteristics of fatigue damage events varied for each flow rate. It was because, though every flow rate had a number of fatigue damage events, but the time and frequency localizations of the events were different for each situation as plotted in Fig. 5 and 6. For the smooth surface, high power spectrums occurred at the normal flow rate where the red stripes exist for a couple of times as shown in Fig. 5. By contrary, the high power spectrums occurred at every flow rate for roughened pipe surface though it happened at different times as shown in Fig. 6. It might be caused by the ununiformity of the surfaces in the roughened pipe. In addition, high power spectrum events occurred more often in the roughened pipe and not depending on the type of flow rates. Obviously in Fig. 5 and 6, the distribution of the high power spectrum happened more frequently across time for roughened pipe compared to the smooth pipe surface.

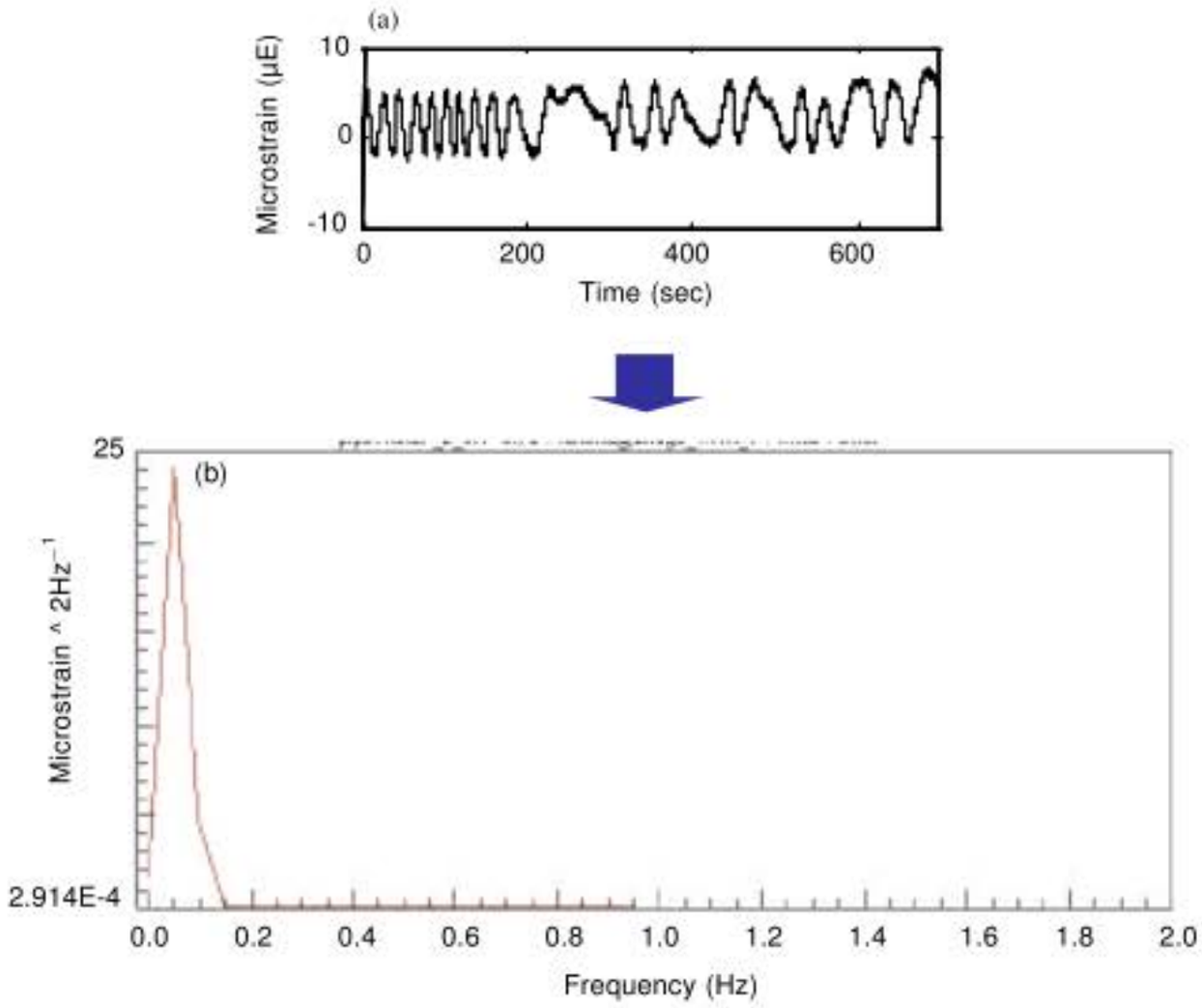

Fig. 3: Signals for roughened surfaced pipe for a normal flow rate: (a) time history and (b) PSD plot

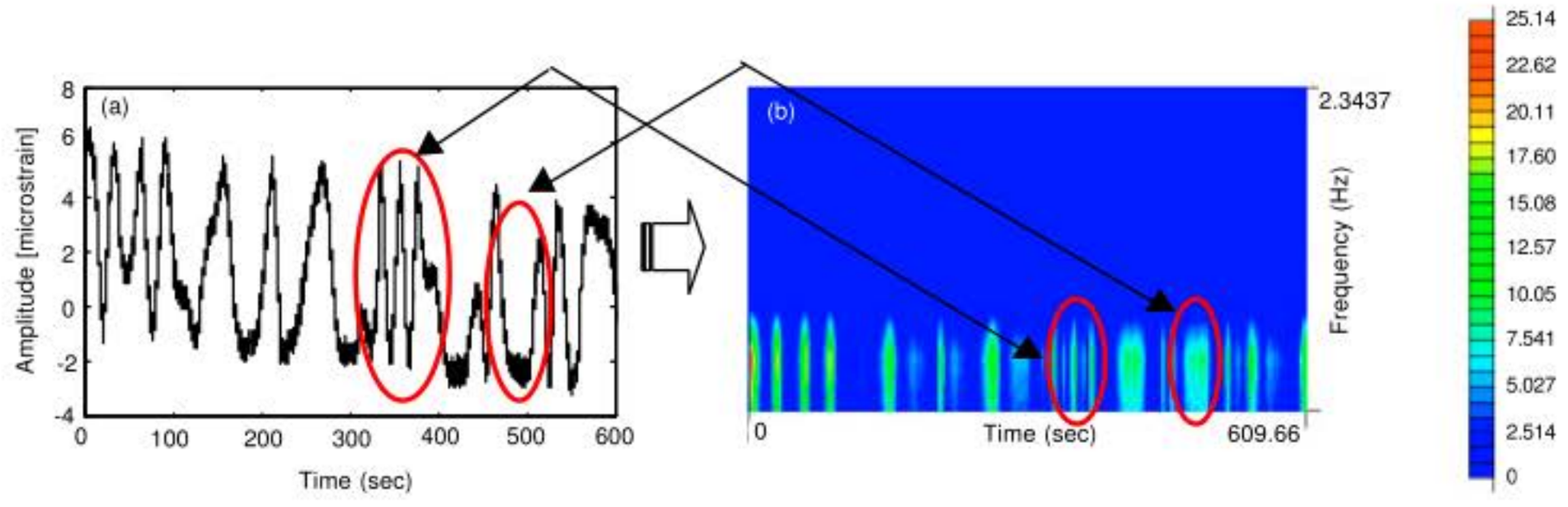

Fig. 4: Representation of smooth pipe signal at the maximum flow rate: (a) time history and (b) STFT

The total of energy was calculated using the power spectrum method which represents the power distribution in the signal as shown in Table 1 and 2. For both of the smooth and roughened pipe surfaces, the highest total of energy occurs at normal flow rate which are 1.060×10^{7} and 0.440×10^{7} $\mu\varepsilon^{2}$ Hz^{-1}, respectively. To our conscious, it appears that the lowest total of energy differs for each pipe surface where it happened at the maximum flow rate for smooth pipe and variable flow rate for the roughened pipe surface.

Table 1: Total of energy for smooth pipe

Flow rate	Total of energy ($\mu\varepsilon^{2}$ Hz^{-1})
Normal	1.060×10^{7}
Maximum	0.212×10^{7}
Variable	0.323×10^{7}

Table 2: Total of energy for roughened pipe

Flow rate	Total of energy ($\mu\varepsilon^{2}$ Hz^{-1})
Normal	0.440×10^{7}
Maximum	0.398×10^{7}
Variable	0.214×10^{7}

Fatigue damage analysis: The strain-life module in GlyphWorks® was utilised to calculate the fatigue damage for smooth and roughened pipe surfaces. The fatigue damage calculation was based on the Smith-Watson-Topper (SWT) relationship in Eq. 3. Thus, the fatigue damage (D) was calculated using Eq. 8:

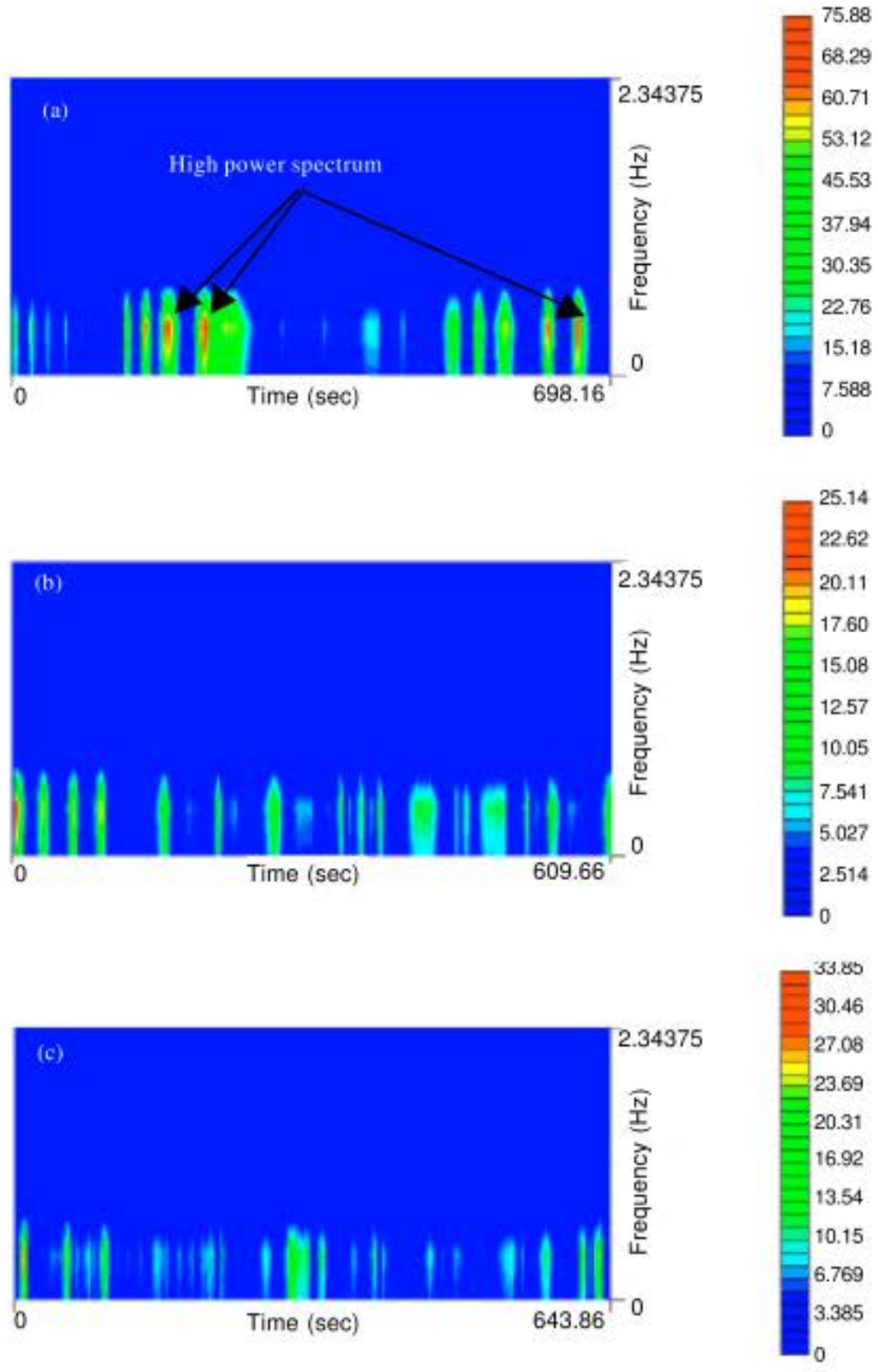

Fig. 5: STFT localization for smooth pipe at different flow rate, (a) normal, (b) maximum and (c) variable

$$D = \frac{1}{N_f} \quad (8)$$

The fatigue damage histogram for smooth pipe surface was shown in Fig. 7, while Fig. 8 showed the fatigue damage histogram for roughened surface pipe at three different flow rates. The red color plot represents the highest value of fatigue damage. Each color of the plot presents different levels of damage which were dark blue is for the lowest, followed by blue, green, yellow, orange and red. There is only low fatigue damage events exist in the smooth pipe surface as shown in Fig. 7. At normal flow rate, there are a number of dark blue plots which represents the low fatigue damage amplitude occur. Gradually, the fatigue damage amplitude increases at maximum and variable flow rates where the light blue plots are more than the dark blue plots. But the amplitude of fatigue damage show an increment in the roughened pipe surface as can be shown in Fig. 8. It is visible to us that the number of fatigue damage events and its amplitude do not exhibit much difference even though the flow rates are different. It showed that fatigue damage amplitude is higher for roughened pipe surface than the smooth pipe. The fatigue damage ratios for both signals are shown in Table 3 and 4. The ratio was calculated with reference to the normal water flow rate. For the smooth pipe surface, the fatigue damage ratio of the maximum and the variable

Table 3: Fatigue damage ratio for smooth pipe

Flow rate	Damage	Ratio (%)
Normal	1.34×10^{-4}	-
Maximum	1.00×10^{-4}	75
Variable	2.53×10^{-4}	189

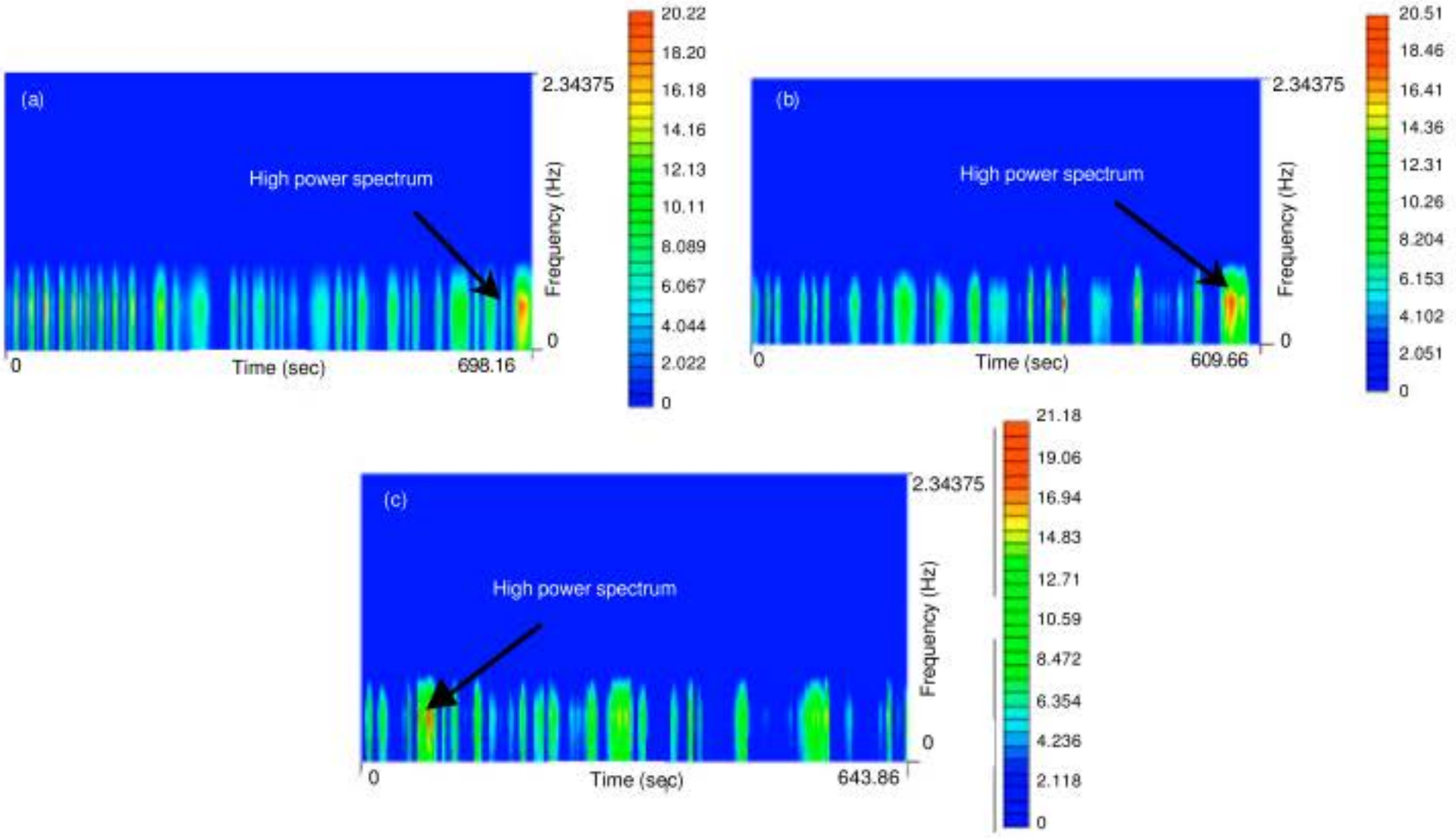

Fig. 6: STFT localisation for roughened pipe at different flow rate: (a) normal, (b) maximum and (c) variable

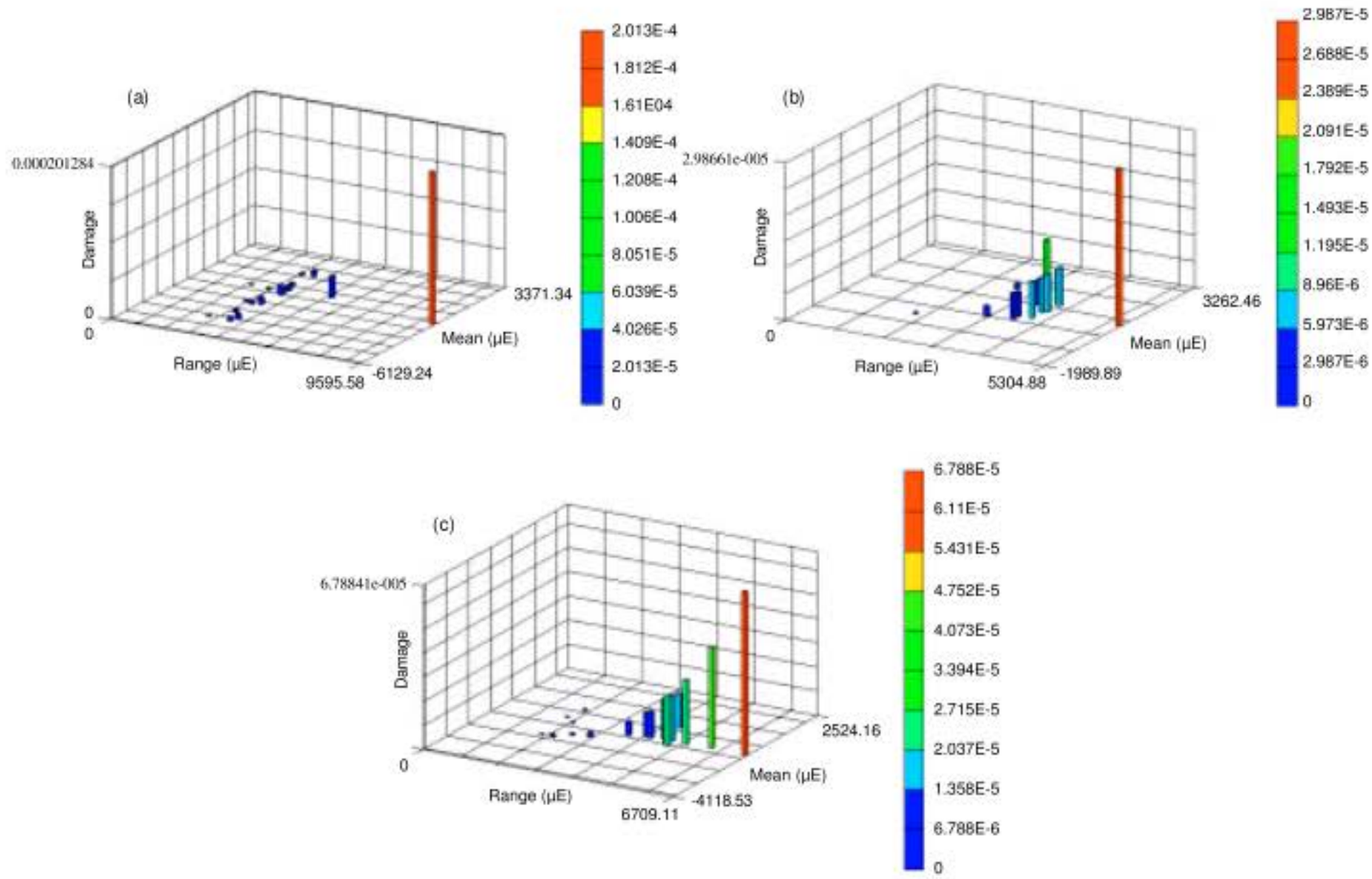

Fig. 7: Fatigue damage histograms for roughened pipe at (a) normal, (b) maximum and (c) variable flow rate

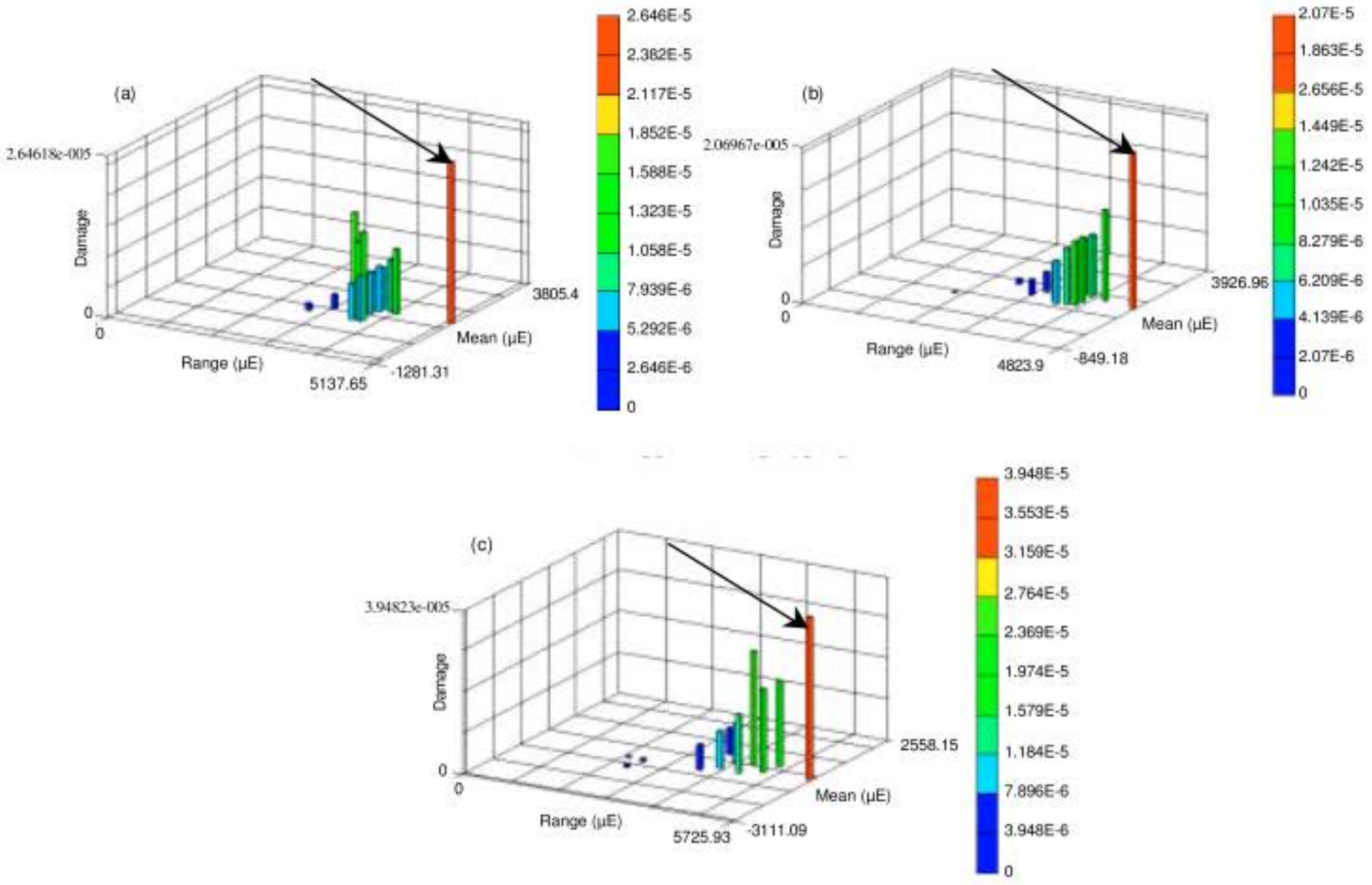

Fig. 8: Fatigue damage histograms for roughened pipe at (a) normal, (b) maximum, (c) variable flow rate

Table 4: Fatigue damage ratio for roughened pipe

Flow rate	Damage	Ratio (%)
Normal	1.51×10^{-4}	-
Maximum	1.02×10^{-4}	68
Variable	1.71×10^{-4}	114

flow rates with respect to normal flow rate was 75% and 189%. It means that the fatigue damage for the maximum flow rate was lower than the normal flow rate. In other words, the fatigue damage value for the variable flow rate is larger than the normal flow rate.

Similar observation can be seen for roughened surface pipe where the fatigue damage ratio of maximum and variable flow rates is 68% of the normal flow rate and 114%, respectively for the normal flow rate.

CONCLUSION

The fatigue damage value obtained for both types of pipe surface indicated that the maximum flow rate contributed to the lowest fatigue damage in the piping system. In the meantime, the fatigue damage ratios at variable flow rate are higher for the smooth and roughened pipe surfaces. From the results, the signal processing approach used in this study was capable in verifying the fatigue damage events in piping system. This study demonstrated the combination approach of signal analysis and fatigue life assessment of piping system in the context of signal patterns and fatigue damage value. By applying the Short Time Fourier Transform (STFT), the fatigue damage events in piping were clarified from the features obtained. This combination could be a very useful tool for the reliable and quick analysis of the structural integrity of piping system.

ACKNOWLEDGMENT

The authors would like to express their gratitude to Universiti Kebangsaan Malaysia and Ministry of Higher Education, Malaysia through the research fundings of UKM-KK-02-FRGS0016-2006 and UKM-KK-02-FRGS0012-2006, for supporting this research.

REFERENCES

Abdullah, S., J.C. Choi, J.A. Giacomin and J.R. Yates, 2005. Bump extraction algorithm for variable amplitude fatigue loading. Int. J. Fatigue, 28: 675-691.

Chui, C.K., 1991. Introduction to Wavelets Academic Press, New York, ISBN: 0121745848.

Dowling, N.E., 1999. Mechanical Behavior of Materials: Engineering Methods for Deformation, Fracture and Fatigue. 2nd Edn., Prentice Hall, New Jersey, ISBN: 0-13-905720-X.

Gokhale, S.R., R. Zoanni, N. Zheng, D.W. Everage and T.H. Hill, 2007. Advances in drillpipe fatigue management. Society of Petroleum Engineers (SPE) Annual Technical Conference and Exhibition, Nov. 11-14, California, USA., pp: 1-1.

Halfpenny, A., 1999. A frequency domain approach for fatigue life estimation from finite element analysis. Proceeding of International Conference on Damage Assessment of Structures (DAMAS 99), Dublin.

Kiymik, M.K., I. Guler, A. Dizibuyuk and M. Akin, 2005. Comparison of STFT and wavelet transform methods in determining epileptic seizure activity in EEG signal for real-time application. Comput. Biol. Med., 35: 603-616.

Lee, Y.L., J. Pan, R.B. Hathaway and M.E. Barkey, 2005. Fatigue Testing and Analysis: Theory and Practice. 1st Edn., Butterworth Heinrahmanemann, New York, ISBN: 978-0-7506-7719-6.

Li, Q., L. Minnetyan and C.C. Chamis, 2001. Computational simulation under PSD fatigue loading. Proceedings of Structures Structural Dynamics and Materials Conference, Apr. 16-19, Seattle, USA., pp: 3147-3154.

Majle, K., H. Purper, B. Wilson, K. Rohler, H. Lehmann, J. Garcia and J. Fernandez, 1996. A new monitoring system for piping systems in fossil fired power plants. Int. J. Pressure Vessels Pip., 66: 305-317.

Miyazaki, K., A. Nebu, M. Ishiwata and K. Hasegawa, 2002. Fracture strength and behavior of carbon steel pipes with local wall thinning subjected to cyclic bending load. Nucl. Eng. Des., 214: 127-136.

Morrow, J., 1968. Fatigue Properties in Metals. In: Fatigue Design Handbook, Section 3.2, Graham, J.A. (Ed.). Society of Automotive Engineers, Inc., Warrendale, PA., pp: 21-29.

Smith, K.N., P. Watson and T.H. Topper, 1970. A stress-strain function for the fatigue of metals. J. Mater., 5: 767-778.

Smith, S.W., 1999. The Scientist and Engineer's Guide to Digital Signal Processing. 2nd Edn., California Technical Publishing, San Diego, ISBN: 0-9660176-3-3.